Size Dependence of the Thin-Shell Model for Carbon Nanotubes

Lifeng Wang,[1] Quanshui Zheng,[1,*] Jefferson Z. Liu,[1] and Qing Jiang[2,*]

[1]*Department of Engineering Mechanics, Tsinghua University, Beijing 100084, People's Republic of China*

[2]*College of Engineering, University of California, Riverside, California 92521-0425, USA*

(Received 19 July 2004; published 1 September 2005)

There has been much debate on the choice for the representative wall thickness for the thin-shell model, although this model has demonstrated remarkable success in capturing many types of behavior of single-walled carbon nanotubes (SWNTs), in determining the buckling strains under compression, torsion, and bending, in particular. This analysis, using the Tersoff-Brenner potential and *ab initio* calculations, shows that the elasticity of the model thin shell evolves from isotropic to square symmetric with the decreasing tube diameter, leading to significant diameter dependence for all the elastic moduli and the representative wall thickness. Furthermore, the elastic moduli of multiwalled carbon nanotubes of diameters up to 10 nm are also size dependent.

DOI: 10.1103/PhysRevLett.95.105501 PACS numbers: 62.25.+g

Much of the research interest in carbon nanotubes was generated by their extreme (e.g., the axial Young's modulus and tensile failure strength) and versatile (semiconducting or metallic, for example) properties. It has been predicted, using molecular dynamics (MD) simulations, tight-binding, and *ab initio* calculations, that carbon nanotubes have an extremely large Young's moduli [1–6], and that their axial failure strains are as high as 16%–24% [2,7,8]. These theoretical predictions have led to continuing efforts to measure the mechanical properties of carbon nanotubes, Young's modulus, in particular, utilizing the behavior of carbon nanotubes in, for example, bending vibration [9,10], bending deflection [11], and axial tension [12]. All these measurements were indirect as Young's modulus was estimated with the measured data, using some well-known relations from the conventional continuum theories of beams and/or tubes, and the use of these relations, inapplicable in many situations [10,13,14], has contributed significantly to the large scattering (0.1–2.0 TPa) of such indirectly measured values of Young's modulus. This has, in part, inspired the contemporary development of continuum models applicable for carbon nanotubes, and notably, Yakobson, Brabec, and Bernholc (YBB) [2] are accredited for developing the continuum thin-shell model for SWNTs. They have modeled a SWNT as a thin shell rolled up from a graphitic monolayer without stretching, and they calculated, using the Tersoff-Brenner potential, the minimum energy by relaxing the rolled structure to its optimized configuration, called the preenergy W_0 of the SWNT, and the excess energy W_1 when the SWNT is subsequently subjected to an axial tensile strain ϵ. They have further equated the second derivative of W_0 with respect to the tube curvature κ and the second derivative of W_1 with respect to the strain ϵ, respectively, to the bending rigidity $D_b = Yh^3/12(1-\nu^2)$ and the tensile rigidity $D_a = Yh$, expressed in terms of the Young's modulus Y, Poisson's ratio ν, and thickness h of a linearly elastic and isotropic thin plate modeling the graphitic monolayer, and they have thus obtained the wall thickness $h = 0.066$ nm, ultrathin compared with the C-C bond length 0.142 nm, and the axial Young's modulus $Y = 5.5$ TPa, unusually large compared with the largest Young's modulus ~ 1 TPa for all previously known materials, as well as the Poisson's ratio $\nu = 0.19$. They have demonstrated remarkable success of this model in capturing many behaviors of SWNTs, in determining the buckling strains under compression, torsion, and bending, in particular, judged by the agreement with their MD simulations using the Tersoff-Brenner potential [2]. We note the earlier work of Robertson *et al.* [1] which shows, using both Tersoff-Brenner potential and first-principles local-density functional methods, that the $1/r^2$ dependence of the preenergy W_0 derived from the linear elastic theory of thin plates remains valid for SWNTs of radii r down to ~ 0.15 nm, and we note that the $1/r^2$ dependence of the preenergy W_0 has also been confirmed by *ab initio* calculations [5,6].

The YBB thin-shell model [2] has generated much debate, centered around the wall thickness of the continuum models for SWNTs, referred to as Yakobson's paradox [15]. Many researchers have modeled MWNTs as assemblies of concentric shells, each modeling a constituent SWNT, and they have taken the average interwall spacing $\bar{s} = 0.34$ nm to be the representative thickness for each of the concentric shells. Setting the thickness $h = 0.34$ nm in the continuum shell model for SWNTs leads to the theoretical prediction that Young's moduli of SWNTs and MWNTs are approximately the same, ~ 1 TPa [3], but the preenergy of such a shell is, however, found to be about 26 times as large as the preenergy of SWNTs calculated using atomistic models. We have noted that the smallest SWNTs are reported to be ~ 0.4 nm in diameter [16]. Furthermore, the high resolution transmission electron microscopy (HRTEM) studies [17,18] show that both SWNTs and MWNTs can sustain severe bending, buckling, kinking, or rippling elastically, leading to the minimum deformation curvature radius estimated as small as

$\sim$0.15 nm, and the corresponding maximum strain $h/2r$, as predicted by the continuum model, would have, however, far exceeded the theoretically predicted fracture strain $\sim$24% of SWNTs, if the wall thickness is taken to be $h = 0.34$ nm. On the other hand, with $h = 0.066$ nm, the corresponding maximum strain is $\sim$22%. There have been some proposals to avoid introducing a thickness [4,15,19], for instance, by introducing the tensile and bending rigidities of SWNTs as two independent mechanical properties [19], not derivable from other elastic moduli, or by modeling a SWNT as a two-dimensional continuum [4,20], instead of three dimensional. Nevertheless, these proposals do not offer the same advantages that the YBB thin-shell model has brought to us because of many well-established theoretical results available in the vast literature for continuum shells [21].

The merits of a continuum model for a nanoscopic system are primarily twofold: (1) consistent in reproducing some basic properties known from reliable *ab initio* calculations or from well-tested semiempirical models (calibration) and (2) convenient in predicting such behaviors that are too expensive, if not prohibitively expensive, to be investigated by reliable *ab initio* calculations or well-established atomistic models. To validate the YBB thin-shell model, we require that the thin-shell model produce the same energies as predicted by an atomistic model [here we have chosen the Tersoff-Brenner potential for the benefit of comparison, as it was used by both Robertson *et al.* [1] and Yakobson *et al.* [2]] for (i) rolling, (ii) uniaxial tension or compression, (iii) radial dilation, and (iv) axial torsion [22], and the same corresponding rigidities. We first reproduced the YBB model values for the axial Young's modulus and wall thickness, by requiring that the thin-shell model produce the same bending and axial tension or compression rigidities as calculated using the Tersoff-Brenner potential. To our surprise, however, the shear modulus $\bar{G}$ derived from these values, using the isotropic elasticity relation $\bar{G} = Y/2(1+\nu)$, is found significantly larger than the shear modulus G obtained by requiring that the thin-shell model lead to the same axial torsion rigidity as calculated using the Tersoff-Brenner potential, and this difference is as large as 18% for SWNTs of diameter 0.4 nm, while the Poisson's ratios obtained from uniaxial and circumferential tensions or compressions exhibit significant dependence upon the chirality. We note that the invalidity of the modulus relation $G = \frac{Y}{2(1+\nu)}$ indicates the breakdown of the elastic isotropy, and we note, on the other hand, that the elastic isotropy is valid for a graphitic monolayer, from which a thin shell is rolled up to model a SWNT in the development of the YBB thin-shell model. To further illustrate this point, we plot in Fig. 1(a) the prestrains ϵ^0_{11} and ϵ^0_{22} of relaxed SWNTs versus the tube diameter predicted by the Tersoff-Brenner potential, namely, the axial and circumferential relative structural change reference to their corresponding rolled-up structures, and we observe that the circumferential strain ϵ^0_{22} is one order larger than the axial strain ϵ^0_{11} and is as large as $\sim$3% for small SWNTs. We note that our results show no chirality dependence in the characteristics of rolling-induced structural changes. It is known that the tangent Young's modulus of a graphitic monolayer with a tensile strain of 3% is about 25% smaller than that without strains. This has therefore motivated us to validate the thin-shell model of SWNTs by considering orthotropic symmetry, instead of isotropic symmetry, with the axial and circumferential directions being privileged. Correspondingly, the in-shell strains ϵ_{ij} and stresses σ_{ij} are related by $\epsilon_{11} = \sigma_{11}/Y - \nu^*\sigma_{22}/Y^*$, $\epsilon_{22} = \sigma_{22}/Y^* - \nu\sigma_{11}/Y$, and $2\epsilon_{12} = \sigma_{12}/G$, with five independent elastic moduli, i.e., the axial and circumferential Young's moduli Y and Y^*, the shear modulus G, and the two Poisson's ratios ν and ν^*.

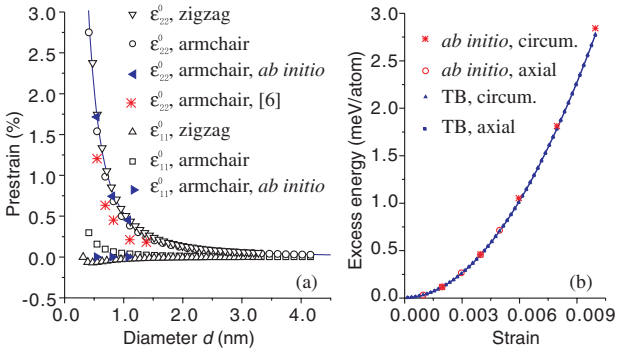

FIG. 1 (color online). *Ab initio* validation for the TB-potential molecular dynamics simulations: (a) Prestrains of relaxed SWNTs. (b) Excess energies vs axial and circumferential extensions for the (4, 4) SWNT.

We denote by $W_0(\kappa)$ the calculated preenergy per atom of a SWNT of diameter d or curvature $\kappa = 2/d$ equivalently, and by $1/\omega$ the in-shell area density of atom, i.e., the atoms per in-shell area. By equating the second derivative of $W_0(\kappa)/\omega$ with respect to the curvature to the bending rigidity of the model shell, we obtain

$$\frac{Y^* h^3}{12(1-\nu\nu^*)} = \frac{1}{\omega}\frac{\partial^2 W_0(\kappa)}{\partial \kappa^2}. \tag{1}$$

We note that the wall thickness h and the elastic moduli Y^*, ν and ν^* in (1), as well as those in (2)–(4), are not preassumed to be independent of the tube diameter d and that the bending rigidity is defined in reference to the SWNT itself, instead of the graphitic monolayer. For a SWNT subjected to a prescribed axial strain ϵ without the radial constraint, we calculate the excess energy $W_1(\epsilon)$ per atom and the corresponding circumferential strain ϵ^* and we thus evaluate the Poisson's ratio ν and the axial rigidity Yh, respectively, as follows:

$$\nu = -\lim_{\epsilon=0}\frac{\epsilon^*}{\epsilon}, \qquad Yh = \frac{1}{\omega}\lim_{\epsilon=0}\frac{d^2 W_1(\epsilon)}{d\epsilon^2}. \tag{2}$$

Conversely, for a SWNT subjected to a prescribed radial strain ϵ^* without the axial constraint, we calculate the excess energy $W_2(\epsilon^*)$ per atom and the axial strain ϵ and we compute the Poisson's ratio ν^* and the circumferential rigidity Y^*h as below:

$$\nu^* = -\lim_{\epsilon^*=0} \frac{\epsilon}{\epsilon^*}, \qquad Y^*h = \frac{1}{\omega} \lim_{\epsilon^*=0} \frac{d^2W_2(\epsilon^*)}{d\epsilon^{*2}}. \quad (3)$$

Furthermore, we calculate the excess energy $W_3(\varphi)$ per atom subjected to a prescribed axial torsion angle φ per unit axial length and we invoke the following relation from the continuum theory of cylindric thin shells:

$$\frac{1}{4}Ghd^2\left(1 + \frac{h^2}{d^2}\right) = \frac{1}{\omega} \lim_{\varphi=0} \frac{d^2W_3(\varphi)}{d\varphi^2}. \quad (4)$$

With the calculated energies W_0, W_1, W_2, and W_3 for armchair (n, n), $n = 3, \ldots, 30$, zigzag $(n, 0)$, $n = 4, \ldots, 41$, and 17 randomly chosen chiral SWNTs, we compute all the six model parameters Y, Y^*, G, ν, ν^*, and h using the six relations in (1)–(4) and we plot the results in Figs. 2(a)–2(d). From them we have the following four observations:

(1) The Young's and shear moduli all increase with the increasing diameter, and their limit values $Y_\infty = Y^*_\infty = 5.07$ TPa and $G_\infty = 2.19$ TPa are the same as those of a graphite monolayer. Small tubes can have as much as ~23% smaller shear moduli and ~10% smaller Young's moduli.

(2) The Poisson's ratios and wall thickness are also diameter dependent and their limit values are $\nu_\infty = 0.158$ and $h_\infty = 0.0665$ nm, respectively, compared with the Poisson's ratio 0.165 for graphite. Both the Poisson's ratios and wall thickness can deviate as much as ~7% from their limiting values.

(3) The negligible differences between Y^* and Y and between ν^* and ν for all tubes indicate that SWNTs have the square symmetry, higher than the orthotropy symmetry. The substantial deviation of $\bar{G} = Y/2(1 + \nu)$ from G, as much as ~18% for small tubes, exhibits the strong nonisotropic effect of small SWNTs, although the isotropy is observed for larger SWNTs.

(4) The tube chirality, particularly armchair and zigzag, has notable effect on the Poisson's ratio, but not on the Young's and shear moduli, nor on the wall thickness.

The underlined mechanism for the material symmetry evolution from isotropic to square symmetric and for the associated phenomena observed above is the significant change in structure taking place during rolling, as indicated by the results shown in Fig. 1(a) both from *ab initio* calculations [6] and using the Tersoff-Brenner potential. For further validation of our results from the Tersoff-Brenner potential, we have also performed *ab initio* calculations for three armchair SWNTs (4, 4), (6, 6), and (8, 8) on the density functional theory (DFT) levels, using the local density with the ultrasoft pseudopotentials approximation and the plane-wave basis set [23]. As shown in Fig. 1(a), the structural changes predicted from these calculations agree remarkably well with our results from the Tersoff-Brenner potential. Furthermore, we have compared the energies from *ab initio* calculations with those obtained using the Tersoff-Brenner potential for various SWNTs, and their excellent agreements are illustrated in Fig. 1(b) with the plots of the excess energies versus the axial and circumferential strains for the (4, 4) SWNT. The indifference between the excess energies due to axial and circumferential deformations supports the results stated above that the axial Young's modulus Y and the circumferential Young's modulus Y^* are apparently the same and so are the corresponding two Poisson's ratios. We note the previous observations [1,4,6,24,25] of the increases of the Young's modulus with the increasing tube diameter and the reported variations of Poisson's ratio [24,25].

We note the importance of this size dependence, although it is insignificant for SWNTs of diameters larger than 1.5 nm, because SWNTs are reported to have diam-

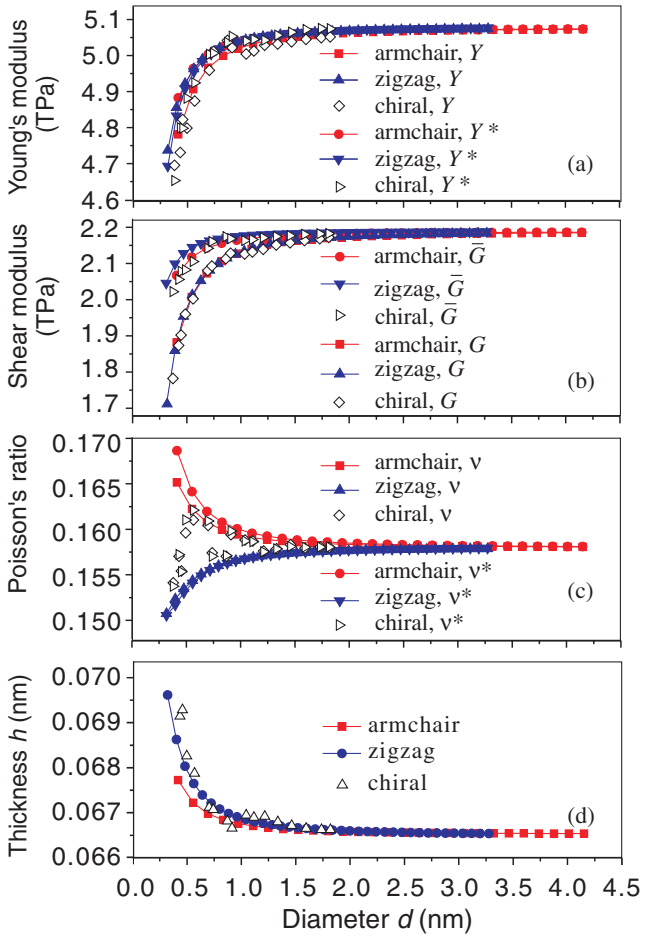

FIG. 2 (color online). Diameter dependence of all the thin-shell model parameters: (a) the axial and circumferential Young's moduli, (b) the shear modulus, (c) Poisson's ratios, and (d) the wall thickness.

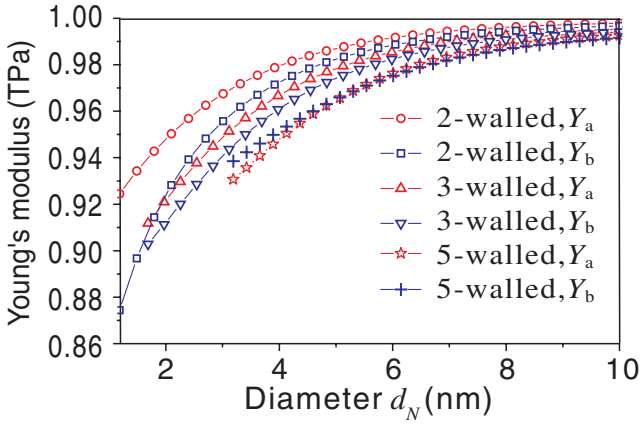

FIG. 3 (color online). Size dependence of axial and bending Young's moduli of MWNTs.

eters typically in the range: 0.4–2 nm, and because it has been shown by MD simulations [26] that larger SWNTs may collapse from the circular to a dumbbell cross section, with the maximal local curvature radius of ~1 nm. We note that larger SWNTs with cylindrical cross sections are stable as constituent components of MWNTs with diameters ranging from 0.4 nm to several tens of nanometers, and we have found, on the other hand, that the mechanical properties of MWNTs exhibit significant size dependence as well, primarily due to the inhomogeneous nature of MWNTs as structural assemblies of SWNTs, such as the reduction of the interwall spacing with the increasing diameter up to ~10 nm [27]. As an illustrative example, let us consider a continuum hollow cylinder of inner and outer diameters d_i and d_o, to model an N-walled carbon nanotube, and we define the axial Young's modulus Y_a and the bending modulus Y_b of this model cylinder by requiring that its axial and bending rigidities, D_a and D_b, be the same as those of the MWNT as a structural assembly of SWNTs. This leads to $Y_a = 4\sum_{j=1}^{N} Y_j h_j d_j/(d_o^2 - d_i^2)$ and $Y_b = 8\sum_{j=1}^{N} Y_j h_j d_j (d_j^2 + h_j^2)/(d_o^4 - d_i^4)$, respectively, with Y_j, d_j, and h_j being the Young's modulus, diameter, and thickness of the jth constituent SWNT. There have been discussions [28,29] on the choices for the inner and outer diameters d_i and d_o, notably (i) setting d_i and d_o to be the measured diameters d_1 and d_N of the innermost and outermost constituent shells of the MWNT, as was done in many experimental reports [9], or (ii) setting $d_i = d_1 - \bar{s}$ and $d_o = d_N + \bar{s}$ with $\bar{s} = 0.34$ nm, and on the variations of the so-derived properties of MWNTs with the wall number. We show in Fig. 3, using the observed dependence of interwall spacing versus diameter [27], that both Y_a and Y_b exhibit the size dependence for MWNTs of diameters up to ~10 nm, regardless of the choice for the diameters d_i and d_o.

We conclude this Letter by pointing out that the thin-shell model of SWNTs have helped to reproduce many complex mechanical phenomena of carbon nanotubes observed in experiments, such as buckling of SWNT [2], unstable behavior or phase transformations of SWNT bundles [30], and bending and torsional ripples of MWNTs [14,31], and may guide to create new structural materials that have unusual or multifunctional properties.

We acknowledge the support of the Chinese NSF Grants No. 10172051, No. 10252001, and No. 10332020, the 973-Project No. G2003CB615603, the Ministry of Education of China, and the U.S. NSF Grant No. CMS-0140568.

*Corresponding authors.
Electronic address: zhengqs@tsinghua.edu.cn
Electronic address: qjiang@engr.ucr.edu

[1] D. H. Robertson *et al.*, Phys. Rev. B **45**, 12592 (1992).
[2] B. I. Yakobson *et al.*, Phys. Rev. Lett. **76**, 2511 (1996).
[3] J. P. Lu, Phys. Rev. Lett. **79**, 1297 (1997).
[4] E. Hernández *et al.*, Phys. Rev. Lett. **80**, 4502 (1998).
[5] J. Kürti *et al.*, Phys. Rev. B **58**, R8869 (1998).
[6] D. Sánchez-Portal *et al.*, Phys. Rev. B **59**, 12678 (1999).
[7] T. Belytschko *et al.*, Phys. Rev. B **65**, 235430 (2002).
[8] T. Dumitrica *et al.*, J. Chem. Phys. **118**, 9485 (2003); Appl. Phys. Lett. **84**, 2775 (2004).
[9] M. M. J. Treacy *et al.*, Nature (London) **381**, 678 (1996).
[10] P. Poncharal *et al.*, Science **283**, 1513 (1999).
[11] E. W. Wong *et al.*, Science **277**, 1971 (1997).
[12] M. F. Yu *et al.*, Science **287**, 637 (2000).
[13] J. Z. Liu *et al.*, Phys. Rev. Lett. **86**, 4843 (2001); Phys. Rev. B **67**, 075414 (2003).
[14] M. Arroyo and T. Belytschko, Phys. Rev. Lett. **91**, 215505 (2003).
[15] O. A. Shenderova *et al.*, Crit. Rev. Solid State Mater. Sci. **27**, 227 (2002).
[16] N. Wang *et al.*, Nature (London) **408**, 50 (2000).
[17] S. Iijima *et al.*, J. Chem. Phys. **104**, 2089 (1996).
[18] M. R. Falvo *et al.*, Nature (London) **389**, 582 (1997).
[19] C. Q. Ru, Phys. Rev. B **62**, 9973 (2000).
[20] B. I. Yakobson and P. Avouris, Top. Appl. Phys. **80**, 287 (2001).
[21] N. Yamaki, *Elastic Stability of Circular Cylindrical Shells* (North-Holland, Amsterdam, 1984).
[22] These are the only four types of deformation that preserve the cylindrical symmetry and thus can be accurately calculated.
[23] M. C. Payne *et al.*, Rev. Mod. Phys. **64**, 1045 (1992); V. Zólyomi and J. Kürti, Phys. Rev. B **70**, 85403 (2004).
[24] V. N. Popov *et al.*, Phys. Rev. B **61**, 3078 (2000).
[25] T. C. Chang and H. J. Gao, J. Mech. Phys. Solids **51**, 1059 (2003).
[26] G. H. Gao *et al.*, Nanotechnology **9**, 184 (1998).
[27] C. H. Kiang *et al.*, Phys. Rev. Lett. **81**, 1869 (1998).
[28] B. I. Yakobson and R. E. Smalley, Am. Sci. **85**, 324 (1997).
[29] S. Govindjee and J. L. Sackman, Solid State Commun. **110**, 227 (1999).
[30] J. Z. Liu *et al.*, J. Mech. Phys. Solids **53**, 123 (2005).
[31] A. Pantano *et al.*, Phys. Rev. Lett. **91**, 145504 (2003).